

Available online at www.sciencedirect.com**SciVerse ScienceDirect**

Procedia Materials Science 1 (2012) 351 – 358

Procedia
Materials Sciencewww.elsevier.com/locate/procedia11th International Congress on Metallurgy & Materials SAM/CONAMET 2011.

Production and Characterization of Glass Microspheres for Hepatic Cancer Treatment

M. B. Bortot^a, S. Prastalo^b, M. Prado^{a,b,c*}^a*Instituto Balseiro, Universidad Nacional de Cuyo Comisión Nacional de Energía Atómica*^b*Departamento Materiales Nucleares, Centro Atómico Bariloche Comisión Nacional de Energía Atómica, Km.9.5Av E. Bustillo, Bariloche 8400, Argentina*^c*CONICET, Consejo Nacional de Investigaciones Científicas y Técnicas, Avda. Rivadavia 1917, Ciudad Autónoma de Buenos Aires C1033AAJ, Argentina.*

Abstract

A simple theoretical mathematical model was developed to assess the process of glass particles spheroidization in a propane-butane-oxygen flame. The model has been designed to gain a better understanding of the dependency amongst the variables that come into play during glass spheroidization. Using the model and theoretical values of: glass viscosity, density, shear modulus, thermal conductivity as well as measured values of the temperature of the flame at different positions, particle size and the vitreous transition temperature, the particle's time-temperature history was calculated inside the flame for different particle sizes and trajectories. For yttrium aluminosilicate (YAS) glass microspheres, of diameter size: 20-50 microns, it was found that the spheroidization process is completed within the flame in short time intervals in the order of 4×10^{-3} to 9×10^{-3} seconds, depending on its thermal trajectory and size of the particle. In this paper the trajectories, degree of spheroidization, temperature variations and velocities of different particle sizes are shown. Using the results obtained from the model, YAS glass microspheres were produced and characterized. Density measurements were done using Helium Pycnometry, chemical composition was studied by Energy Dispersive Spectroscopy. The microsphere surface was characterized using Scanning Electron Microscopy and the glass was thermally characterized by means of Differential Thermal Analysis.

* Corresponding author. Tel.: +54-294-4445241
E-mail address: pradom@cab.cnea.gov.ar

© 2012 Published by Elsevier Ltd. Selection and/or peer-review under responsibility of SAM/ CONAMET 2011, Rosario, Argentina.

Keywords: Spheroidization; Yttrium Aluminosilicate Glass; Glass Microspheres

1. Introduction

Liver cancer happens to be the third most common type of cancer in the world that leads to death. In the case of inoperable liver cancer it has been shown that the treatment of internal selective radiotherapy with radioactive glass microspheres extends and improves the patient's life quality www.nordion.com/therasphere/. In this work, glass microspheres were obtained using yttrium aluminosilicate glass particles of this specific composition $45\text{Y}_2\text{O}_3:20\text{Al}_2\text{O}_3:\text{Si}_2\text{O}$ (%wt). The glass particles were obtained by milling glass and then sieving the particles to obtain a 25-50 microns particle size distribution. The selected particles were then spheroidized in a propane-butane-oxygen flame that has a temperature distribution from 600°C up to 2000°C .

During the particle's trajectory inside the flame the glass particles decrease their viscosity and due to the effects of surface tension the particles develop a spherical shape. Once the microspheres are obtained they are sent to a nuclear reactor to be activated, where the ^{89}Y that forms part of the glassy matrix becomes ^{90}Y by neutron absorption. ^{90}Y is a beta emitter radioisotope, and has been proved to be useful for internal selective radiotherapy therapy of liver cancer. To be able to increase the production of microspheres and to generate a reproducible process it is important to identify the parameters that influence and modify the obtained results. The main variables that were identified consist of: a) physical properties of the glass material such as density, glass viscosity, thermal conductivity, particle size b) properties of the flame: temperature profile, gas velocity c) process parameters: geometry and particle feed rate into the flame. As means to study the spheroidization process during the thermal trajectory of the particle, a simple physical-mathematical model was developed. The model basically consists in following the trajectory of each particle, adding the fractions of glass relaxation time in each time interval. When the addition of the fractions reaches 1 (or 100 in this case) spheroidization has been achieved. The model does not focus on the combustion process or the fluid dynamics involved with flame propagation, the aim of the model is to analyze the variables that come into play during the spheroidization process. The main aspects that need to be considered when designing the spheroidization process are the requirements that the resulting microspheres need to fulfill. The microspheres used for the treatment need to have a diameter that falls within 20-50 microns range so that they can be embolized within the tumor microvasculature. Since, Yttrium, the beta emitting radionuclide has maximum and average emissions of 2.28MeV and 933.7KeV respectively with maximum and average path lengths in tissue of 11 and 2.5 mm then most of the absorbed dose deposition will occur in a limited area in proximity to the tumor and hence a selective treatment is obtained Gulec 2010. Simultaneously, high sphericity, smooth surface, absence of crystallization and good lixiviation resistance are other characteristics that have to be taken into account during the production process.

Using the results obtained from the simulation it was concluded that for a particle to reach spheroidization it must fall within a certain region of flame in proximity to the burner. A vibratory glass particle feeder was designed so as to direct the particles towards the hot area of the flame minimizing the amount of glass particles that do not achieve full spheroidization. However, a certain percentage of the microspheres obtained were found to have a diameter greater than 50 microns. This could be attributed to two factors: the presence of initial acicular particles with sizes greater than 50 microns and gas bubbles within the spheres. The microspheres that contained inner gas bubbles were subjected to a second spheroidization to determine whether a second thermal trajectory would aid in the elimination of the gasses found within the glass microspheres. To evaluate the effect of a second spheroidization, the glass particles as well as the

microspheres were subjected to Differential Thermal Analysis tests, X-Ray Diffraction analysis and chemical analysis using Energy Dispersive Spectroscopy.

Nomenclature

C_d	Particle drag coefficient
r_p	Particle radius
d_p	Particle diameter
ρ_p	Particle density
ρ_{gc}	Combustion gas density
ρ_{gases}	Gas density
V_p	Particle velocity
V_{gc}	Combustion gas velocity
V_{gases}	Gas velocity
P_{total}	Stagnation pressure (Total pressure)
C_p	Specific heat capacity
T_s	Temperature of the sphere
T_p	Temperature of the particle
Nu	Nusselt number
K_f	Thermal conductivity
σ	Stefan Boltzmann constant
ε	Emissivity
η	Viscosity
τ_R	Relaxation time
T_i	Temperature at time i
Δt_i	Time interval
T_g	Glass transition temperature

1.1. Flame spheroidization model

A calculation code was written to perform the mathematical analysis based on the following equations. The equations in the work of Ozturk et.al 2006 were adapted in order to obtain the particle's trajectories within the flame. The acceleration of the particle in x-direction (the x-direction which coincides with the axis of symmetry of the flame) was calculated by eq.(1) and the acceleration in y-direction (which is in the direction of the gravitational force) by equation (2).

$$\frac{dV_x}{dt} = \frac{3C_D}{8r_p} \frac{\rho_{gc}}{\rho_p} \left(\left| V_{gc} - V_p \right| \right) \left(V_{gc} - V_p \right) \quad (1)$$

$$\frac{dV_y}{dt} = -\frac{3C_D}{8r_p} \frac{\rho_{gc}}{\rho_p} \left(\frac{V^2}{P} \right) + g \quad (2)$$

In the model the value of the drag coefficient depends on the value of Reynolds number Hossain 2007. It was assumed that the propane-oxygen gas mixture begins to combust instantly after it has gone through the orifices of the burner. The pressure of the gasses at that instant (stagnation pressure, eq.3a) is slightly above atmospheric pressure. Assuming it is being dealt with an incompressible flow of variable properties, the relationship mentioned in eq. (3) for dynamic pressure can be used. At the same time, by observing the flame it was concluded that approximately 30 cm away from the burner, the velocity of the flame gases were almost null. Applying these assumptions, equations (3) and (4) were developed.

$$P_{total} = P_{atm} + \frac{1}{2} \rho_{gases} V_{gases}^2 \quad (3a) \quad P_{total}(x) = P_{atm} + \Delta P \left(1 - \frac{x}{30} \right) \quad (3b)$$

$$V_{gasCombustion} = \sqrt{2 \times \rho_{gasCombustion} (P_{total} - P_{atm})} \quad (4)$$

Temperature measurements were taken at different positions within the flame with a platinum-rhodium-platinum thermocouple. The values collected were used to interpolate for intermediate positions and hence solve for the whole flame temperature profile. Based on this analysis it is assumed that the fluids that exert a force on the particle in x-direction are the combustion gases. The temperature range of interest is above the glass transition temperature T_g , and it is presumed that under these conditions the water present as a flame combustion product is dissociated in the form of oxygen and hydrogen. The properties of these substances at different temperatures were obtained from tables from Incropera et al. 2007, to solve eqn. (4) at different positions within the flame. After solving for the gas velocity in x-direction, calculations were performed to solve for the particle's acceleration in x-direction. Given that, it was assumed that the combustion gases only have momentum in x-direction, the equation for acceleration in y-direction needs a different analysis. From the values of acceleration in both directions, total velocity was calculated and the resulting particle trajectory. Relating the particle's position to the temperature of the flame at each instant eqn. (5) was used to solve for the values of temperature of the particle. Using the theoretical viscosity as a function of temperature values established through Priven's 2000 method (SciGlass 6.6) and adjusted using the equation of Vogel-Fulcher-Tamman the particle viscosity value at each instant was approximated. From the equations that describe the rheological properties of high viscosity fluids developed by Maxwell, Kelvin and Voight, the relaxation time of a viscous fluid is related to the viscosity as shown in eqn. (6)

$$\frac{1}{6} \pi d_p^3 \rho_p C_p \frac{dT_p}{dt} = Nu \frac{K_f}{d_p} (T_p - T_s) \pi d_p^2 - \sigma T_p^4 \pi d_p^2 \quad (5)$$

$$\tau_r = \frac{\eta}{G^*} \quad (6) \quad \text{spheroidization} = 100 \sum_i \frac{\Delta t_i G^*}{\eta(T_i)} \quad (7)$$

The proportionality factor G^* has dimensions and physical meaning of shear modulus as referred to in Gutzow et.al.1997. The spheroidization index was calculated by equation 7. The equation 7 states that at the i -th time interval (term Δt_i) the particle is subjected to a temperature T_i and the its viscosity value during that interval is $\eta(T_i)$. Hence, when equation 7 is equal to 100 the spheroidization process is complete.

2. Production and characterization of bulk glass and glass microspheres

Yttrium, alumina and silica $45\text{Y}_2\text{O}_3:20\text{Al}_2\text{O}_3:\text{Si}_2\text{O}$ (%wt) were mixed and homogenized. The powders were placed in a platinum crucible during two hours at 1600°C and later vitrified using the splat cooling technique. The glass was then milled and sieved to separate the particle range of interest that lies between 25-36 microns. The particles were then spheroidized in a propane-butane-oxygen flame. The particle size distribution was measured using optical microscopy. The X-Ray Diffraction analysis was carried out using a Philips Powder Diffractometer, model PW 1700 equipped with a graphite monochromator. The microspheres were also analyzed using a Scanning Electron Microscope Philips 515 equipped with EDAX spectrometers 9900 and Micropex WDX for Energy Dispersive Spectroscopy (EDS).

2. Results and Discussion

3.1 Thermal trajectory and particle spheroidization

The model was used to calculate the spheroidization of particles of different sizes during different trajectories, simulating also different points of entry of the particles in the flame.

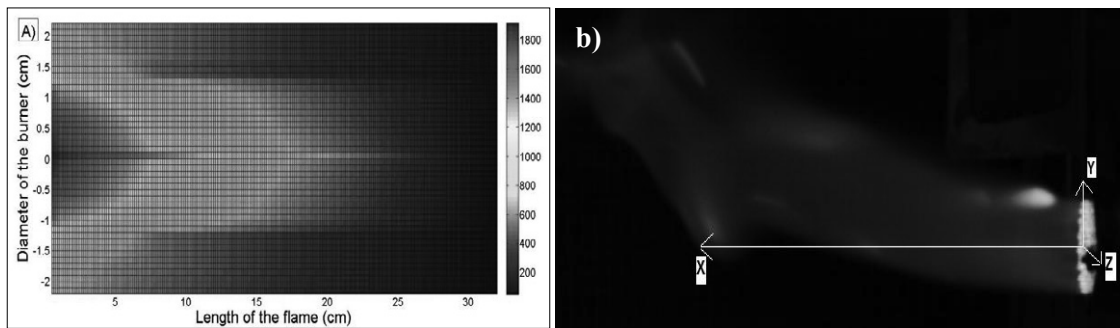


Fig 1 (a) Flame temperature profile; (b) Image of the flame and the axes

The spheroidization of the particle depends on the time spent within the flame τ_R , with a viscosity value low enough (or high enough temperature) so that by effect of surface tension a sphere is formed. Because of this reason the model contributed to defining that the amount of time of the particle in the flame is not the main variable but rather the temperature-time combination to which the particle is subjected to. The particles with sizes greater than 200 microns were not spheroidized as can be observed in Figure 2(b) and 3(b). Given that these particles have greater mass, the particle travels a smaller trajectory in the flame and the heat exchange kinetics does not allow the particle to reach a temperature higher than the value of T_g , and because of this reason the particle does not reach a complete spherical shape. On the other hand, the smaller particles, the ones close to 20 microns are also greatly affected by a higher initial acceleration when they enter the flame. The flame limits exhibit greater temperature fluctuations as can be observed in Figure 2 (a) and this generates variations in the particle's temperature and velocity. Smaller particles show a "surfing effect", they have a trajectory that runs by the upper limits of the flame, through low temperatures even below T_g .

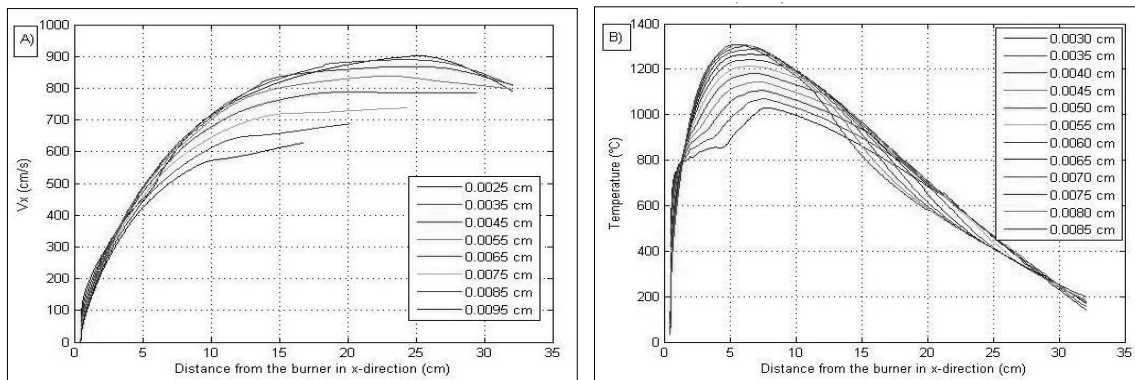


Fig 2 (a) Particle velocity in x-direction with respect to distance from the burner ; (b)Temperature of the particle with respect to distance from the burner within the flame.

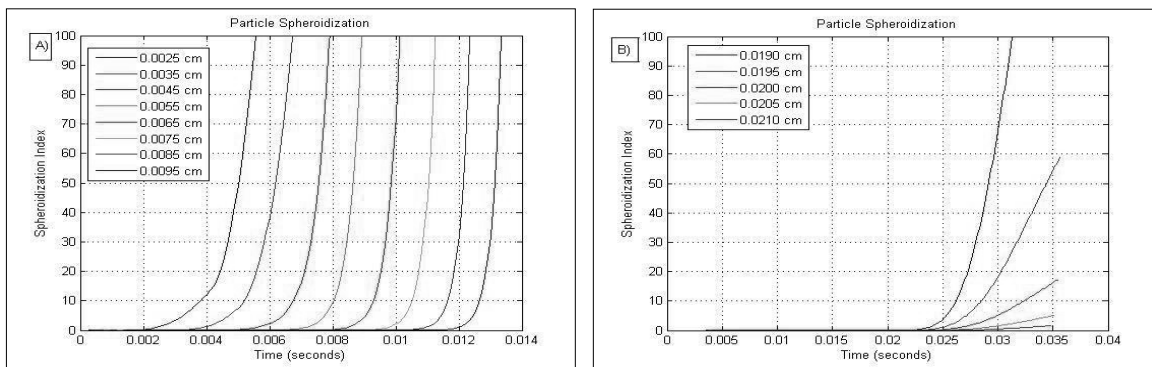


Fig 3 (a) Spheroidization times for spheres of sizes smaller than 95 microns; (b) Spheroidization times for sizes >190 microns

Figure 4 (a) shows microspheres within the 25-70 microns particle size range. The microspheres of a greater diameter size range exhibit the presence of gas bubbles as well as numerous surface and geometrical imperfections.

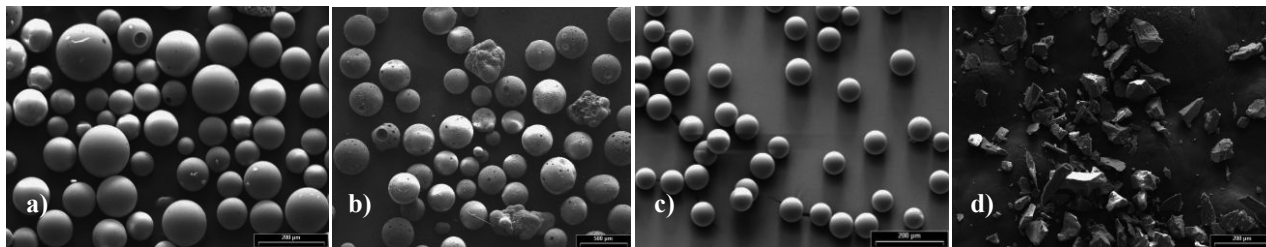


Fig 4 Experimental results that validate the model (a) Microspheres with size distribution smaller than 200 microns (b) Microspheres with diameter size bigger than 200 microns (c) Narrow microsphere size distribution (smaller than 100 microns) (d) Irregular particles before spheroidization

In the case of Figure 4 (b) because of greater initial particle size the resulting microsphere size varies between 200-400 microns and as predicted in Figure 3(b) the spheroidization process does not reach completion. The model was also used to simulate and study the entry of the particles in different points across the diameter of the burner. Considering the z-axis as the horizontal axis across the diameter of the burner it was observed that particles sized within the 20-45 micron range did not reach spheroidization when they

entered the flame a distance of 1,15 cm away from the center of the burner. Because of this reason the feeding system was modified. The bottom area of the particle feeder was reduced so that the particles would be directed and would fall within a range of $\pm 5\text{mm}$ of the axis of symmetry of the flame which assured that all the particles within the adequate particle size range would spherodize. The particle size distribution obtained can be observed in Figure 6.

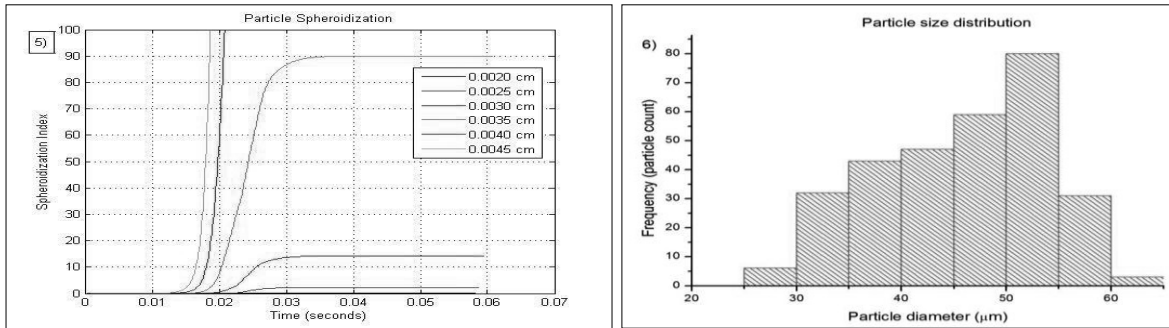


Fig. 5 Spheroidization index and time of particles fall 1,1 cm away from the center of the burner; Fig. 6 Microsphere particle size distribution

The yttrium concentration within the microspheres was analyzed by EDS. Composition measurements were done starting from the surface towards the interior of the sphere every 10 microns and the results showed that there was a slight increase of yttrium concentration towards the surface. At the same time, helium pycnometry measurements were taken to study whether the density of the microspheres would change after a second spheroidization, the objective was to see if there was a reduction of gases present within the spheres that would cause an increase in density. The expected density increase, was not observed, however the results fall within the error of the measurement. The values obtained are recorded in Table 1.

Table 1. Helium pycnometry results of the different samples

Sample	Mass (gr)	Density (He)(g.cm ⁻³)
YAS glass particles	0,97	3,47±0,04
1 Spheroidization	1,21	3,27±0,02
2 Spheroidizations	1,24	3,35±0,04

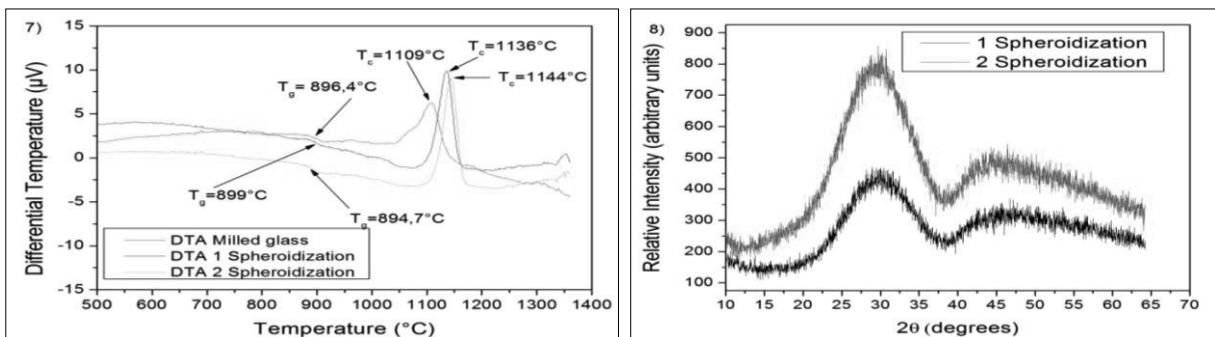


Fig. 7 Differential Thermal Analysis results of the different samples; Fig. 8 X-Ray Diffraction results of microspheres (1 and 2 spheroidizations)

The vitreous transition values and crystallization temperatures were obtained as can be observed in Figure 7. The results obtained show that the crystallization temperature increases for the microspheres, this occurs due to the fact that microspheres present fewer surface defects, and hence a smaller number of nucleation sites from where crystallization can start in comparison to milled glass particles. X-Ray Diffraction analysis was also conducted for the three samples and as can be seen from Figure 8 no crystalline phase was detected. These results are reasonable given that the time the particles spent on and above the crystallization temperature is very small, in the order of milliseconds.

3. Conclusion

A simple model to study irregular glass particle spheroidization in a propane-butane-oxygen flame was developed. Using the results obtained from the model it was confirmed that the spheroidization of the particles depend on the particle size and the position where the particle enters the flame. In some cases the thermal trajectory does not allow the particle to reach the temperature of vitreous transition and the particle does not spheroidize. At the same time, the results obtained explained the reason why when using glass particles that have lower density values and smaller size distributions these seem to "float" on the edge of the flame. Depending on the density-size relationship of the particle in some cases the glass powder does not penetrate within the flame and which means that it does not reach the hot zone and the particles do not spheroidize. Taking into account the results obtained from the calculations, YAS microspheres of different sizes were produced. In regards to crystallization, it was found that although the temperature that the microspheres reach within the flame goes beyond the glass crystallization temperature (measured using DTA) the microspheres do not crystallize. Crystallization is avoided because the residence time of the microspheres at high temperatures is in the order of 0.01 s (too short for crystallization to take place) and the fast cooling rates prevent the crystallization phase transformation.

Acknowledgements

The Authors thank Nicolas Silin who helped with the design of the model and Silvina Pérez Fornells.

References

- Gulec S.A., Szejnberg M.L., Siegel J.A., Jevremovic T., Stabin M., 2010. Hepatic Structural Dosimetry in 90Y Microsphere Treatment: A Monte Carlo Modeling Approach Based on Lobular Microanatomy, *Journal Nuclear Medicine* 51, p.301-310
- Gutzow I., Schmelzer J., 1995. *The Vitreous State*, Springer-Verlag Heidelberg
- Hossain M.M., Yao Y., Watanabe W., 2007. A numerical Study of Plasma-Particle energy Exchange Dynamics in Induction Thermal Plasmas for Gasification, *Materials Science and Technology*, p.393-401
- Hu P., Yan S., Yuan F., Bai L., Li J., Chen Y., 2007. Effect of Plasma Spheroidization Process on the Microstr. and Cryst. Phases of Silica, Alumina and Nickel Particles, *Plasma Sc. and Tech.*, Vol.9, No.5
<http://globocan.iarc.fr/>
- Incropera, DeWitt, Bergman L., 2007. *Fund. of Heat and Mass Transfer*, John Wiley & Sons. p. 260–261
- Ozturk A., Cetegen B.M., 2006. Modeling of precipitate formation in precursor droplets injected axially into an oxygen/acetylene combustion flame, *Journal of Materials Science and Engineering A* 422, p. 163-175.
- SciGlass 6.6, ITC, Institute of Theoretical Chemistry, Newton, MA 20459.
- Zhang T., Gawne D.T., Liu B., 2000. Computer modeling of the influence of process parameters on the heating and acceleration of particles during plasma spraying, *Surface and Coatings Technology* 132, p. 233-243.